

Simulations of Atmospheric General Circulations of Earth-like Planets by AFES

Project Representative

Yoshi-Yuki Hayashi Department of Earth and Planetary Sciences, Kobe University

Authors

Yoshi-Yuki Hayashi^{*1}, Yoshiyuki O. Takahashi^{*1}, Norihiko Sugimoto^{*2}, Masahiro Takagi^{*3}, Masaki Ishiwatari^{*4}, Masatsugu Odaka^{*4}, Shinichi Takehiro^{*5}, Kensuke Nakajima^{*6}, George L. Hashimoto^{*7} and Yoshihisa Matsuda^{*8}

*1 Department of Earth and Planetary Sciences, Kobe University

*2 Research and Education Center for Natural Sciences, Keio University

*3 Department of Earth and Planetary Science, The University of Tokyo

*4 Department of CosmoSciences, Hokkaido University

*5 Research Institute for Mathematical Sciences, Kyoto University

*6 Department of Earth and Planetary Sciences, Kyushu University

*7 Department of Earth Sciences, Okayama University

*8 Faculty of Education, Tokyo Gakugei University

High resolution simulations of the Martian atmosphere have been performed by using a General Circulation Model (GCM) based on AFES (Atmospheric GCM for the Earth Simulator). Also performed is a simulation of the Venus atmosphere by using AFES with simplified physical processes and with a resolution higher than that used by previous studies. Our aim is to have insights into the dynamical features of small and medium scale disturbances in the Earth-like atmospheres and their roles in the general circulations. Mars simulations are performed by the use of quite high horizontal resolution. The results of the long term simulations show that the latitudes and seasonal dates of dust lifting events diagnosed in the high resolution model (T319L96) are qualitatively similar to those in the medium resolution model (T79L96), while representations of disturbances are different between the two resolution simulations. However, as is expected, dust lifting region is larger in high resolution model than in medium resolution model. This implies the importance of effects of small scale disturbances to maintain dust amount in the atmosphere. As for the simulation of the Venus atmosphere, a superrotation is successfully maintained for a long time with including a realistic solar heating. In addition, baroclinic modes grow at the cloud layer where static stability is low. Structures of the unstable modes are similar to those obtained in the linear stability analysis at initial, but their horizontal structures change later. Meridional transport of momentum and heat by these unstable modes is discussed. The present results suggest that (1) the vertical distribution of static stability is crucial for baroclinic instability, (2) baroclinic instability, which has not been reproduced in the previous studies, is likely to take place in the Venus atmosphere, and (3) the baroclinic unstable modes play one of the key roles on the general circulations of the Venus atmosphere.

Keywords: planetary atmospheres, superrotation, dust storm, Earth, Mars, Venus

1. Introduction

The structure of the general circulation differs significantly with each planetary atmosphere. For instance, the atmospheres of the slowly rotating Venus and Titan exemplify the states of superrotation where the equatorial atmospheres rotate faster than the solid planets beneath, while the weak equatorial easterly and the strong mid-latitude westerly jets form in the Earth's troposphere. The global dust storm occurs in some years on Mars, but a similar storm does not exist in the Earth's atmosphere. Understanding physical mechanisms causing such

a variety of features in the general circulations of the planetary atmospheres is one of the most interesting and important open questions of the atmospheric science and fluid dynamics.

The aim of this study is to understand dynamical processes that characterize the structure of each planetary atmosphere by performing simulations of those planetary atmospheres by using GCMs with a common dynamical core of AFES [1]. Appropriate physical processes are adopted for each planetary atmosphere. In our project so far, we have been mainly performing simulations under the condition of Mars. In addition,

the accurate radiation model of the Venus atmosphere has been constructed for the simulations under the condition of Venus. In the followings, the particular targets of each simulation, the physical processes utilized, and the results obtained will be described briefly.

2. Mars simulation

2.1 Targets of simulations

Radiative effect of dust suspended in the Martian atmosphere has important impacts on the thermal and circulation structure of the Martian atmosphere. However, it has not been understood fully what kind of dynamical phenomena play important role in lifting dust from the ground into the atmosphere. A previous study by using a Mars GCM [2] suggests that the effects of wind fluctuations caused by small and medium scale disturbances would be important for the dust lifting processes. However, the features of small and medium scale disturbances which may contribute to the dust lifting have not been clarified. Disturbances of these scales are not easy to be observed and to be resolved in numerical models. In order to examine the disturbances in the Martian atmosphere and its effects on dust lifting, we have been performing medium and high resolution simulations of Martian atmosphere by using a Mars GCM. In this fiscal year, long term simulations are performed to examine the seasonal variation of dust lifting.

2.2 Model and experimental settings

Mars simulations are performed by AFES with the physical processes introduced from the Mars GCM [3, 4] which has been developed in our group, and the values of physical constants appropriate for the Mars. The implemented physical processes are radiative, turbulent mixing, and surface processes. By the use of this AFES, long term simulations are performed. Resolutions of simulations are T79L96 and T319L96, which are equivalent to about 89 and 22 km horizontal grid sizes, respectively. In the simulation performed in this fiscal year, the atmospheric dust distribution is prescribed, and the dust is uniformly distributed

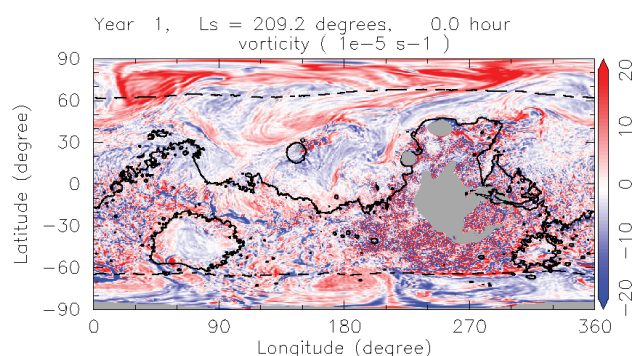


Fig. 1 Global distribution of vorticity at the 4 hPa pressure level at northern fall with the resolution of T319L96. Unit of vorticity is 10^{-5} s^{-1} . Also shown is the areoid (solid line) and low latitude polar cap edge (dashed line). Gray areas represent mountains at the 4 hPa pressure level.

in horizontal direction with an amount corresponding to visible optical depth of 0.2. However, the dust lifting parameterization [5] is included in the model to diagnose the possible amount of dust lifting.

2.3 Results

Figures 1 and 2 show snapshots of global distribution of relative vorticity at the 4 hPa pressure level during the northern fall from T319L96 and T79L96 simulations, respectively. By comparing these vorticity distributions, differences in representation of disturbances between two simulations are observed. Some of those are fine structure of fronts in the mid- and high-latitudes of T319L96 simulation and clear appearance of small scale vortices in the low latitudes of T319L96 simulation.

Here, seasonal variations of dust lifting flux is examined. Figure 3 shows seasonal variations of zonal mean dust mass flux obtained from T319L96 (top) and T79L96 (bottom) simulations. The most important dust lifting events are observed at the northern middle latitudes and the southern low latitudes in the winter. Although the representations of disturbances with different resolutions are different as is shown in Figs. 1 and 2, the latitudes and seasonal dates at which dust lifting events occur are similar between both simulations. However, as is expected, the area of dust lifting regions is larger in T319L96 simulation than T79L96 simulation. This implies the representation of atmospheric disturbances has a significant impact on the initiation and the strength of dust lifting events in the model.

3. Venus simulation

3.1 Targets of simulations

In order to investigate the phenomena such as superrotation in the Venus atmosphere, GCMs with relatively low resolutions have been used so far [6]. In previous GCM studies, since the main purpose of those studies is to reproduce a superrotation itself from a motionless state, extremely long spin-up time is needed. In addition, some of these models include unrealistic solar heating and static stability of the atmosphere to generate a superrotation. In the present study, we construct a new model on

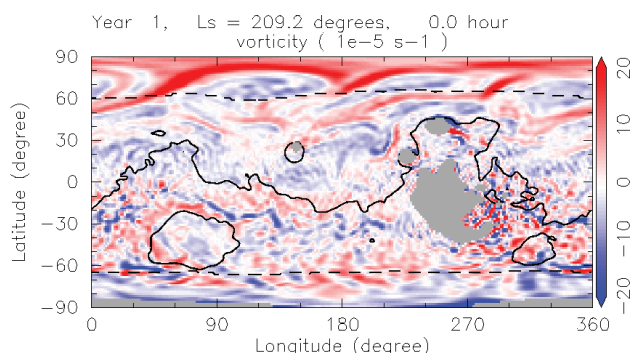


Fig. 2 Same as Fig. 1, but for resolution of T79L96.

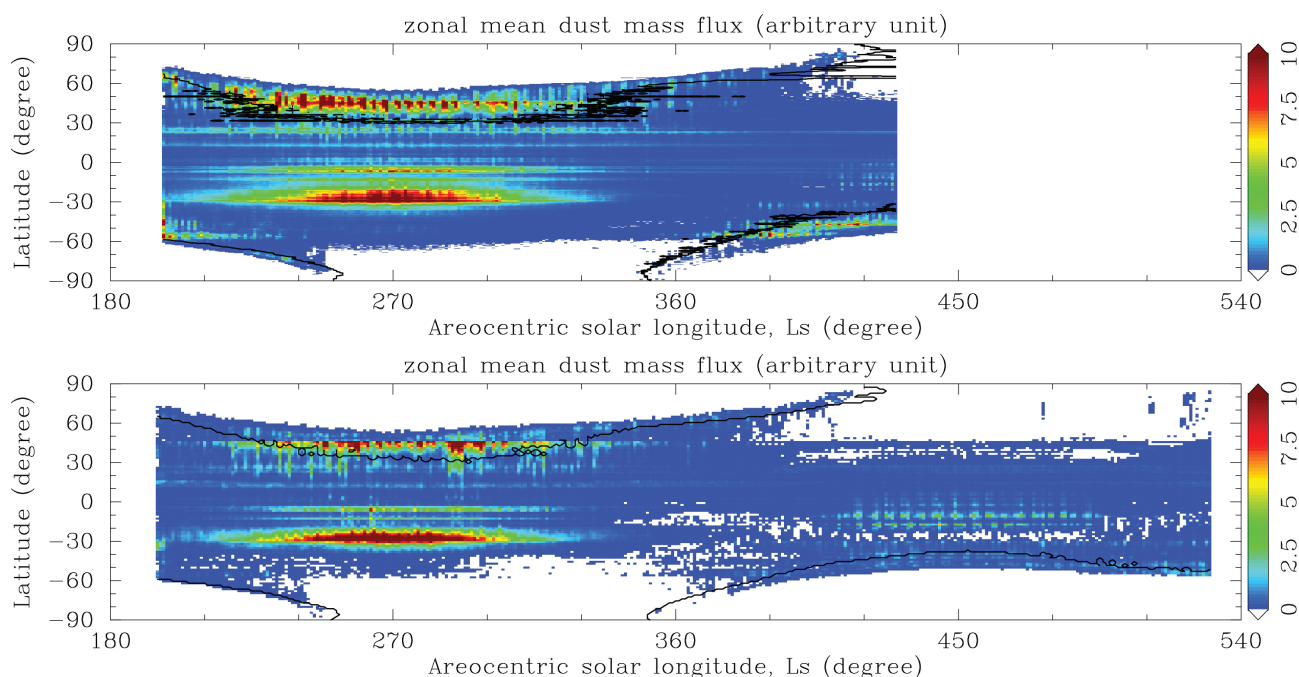


Fig. 3 Seasonal variations of zonal mean normalized dust mass fluxes for T319L96 simulation (top) and T79L96 simulation (bottom). Black solid line indicates the location of polar cap edge. Unit of dust mass flux is arbitrary. Note that the T319L96 simulation is still on going.

the dynamical basis of AFES to realize realistic simulations of the Venus atmosphere. As a first step toward a long-time high-resolution numerical simulation to reproduce a superrotation, we investigate possible unstable modes in the superrotating Venus atmosphere with a realistic profile of static stability.

Linear stability analyses of superrotation [7, 8] suggest that baroclinic modes may grow in the cloud layer with small static stability. However, no observational study directly shows baroclinic instability in the Venus atmosphere so far. The baroclinic unstable modes may have important roles in transporting heat and producing large horizontal eddy viscosity assumed in the Gierasch mechanism [6, 9]. Therefore, it is important to investigate the baroclinic instability in a nonlinear numerical simulation to extend the previous results of the linear stability analyses [10, 11]. We also investigate the dependence of baroclinic instability on the static stability and discuss meridional transport of momentum and heat by the baroclinic modes [12]. Finally, we include a realistic solar heating as a test case [13].

3.2 Model and experimental settings

Venus simulations are performed with simplified physical processes and physical constants appropriate for the Venus. Experimental settings are basically based on the previous linear stability analysis [8]. Physical processes included in the model are vertical eddy diffusion with a constant diffusion coefficient of $0.015 \text{ m}^2/\text{s}$, a dry convective adjustment, Newtonian cooling, and Rayleigh damping at the lowest level to represent the surface friction. In the upper layer above 80 km, a sponge layer is assumed; the friction increasing gradually with height damps the disturbances, but does not act on the zonal-mean

component of the zonal wind. In addition, the model includes 8th order horizontal diffusions (∇^8) with e-folding time of about 0.1 days for the maximum wavenumber. The Newtonian cooling coefficients are based on the previous study [14]. The equilibrium temperature distribution toward which temperature is relaxed by Newtonian cooling is the initial value described below. In addition we also prepare cases with the realistic solar heatings which have a vertical profile based on the previous works [14, 15] as a test case. Two simulations are performed; one is the case with a zonally averaged solar heating, and the other is the case with diurnal variation.

The resolution used in the present simulations is T42L60, which has 128 and 64 grids in the longitudinal and latitudinal directions, respectively. Vertical domain extends from the ground to about 120 km with almost the constant grid spacing of 2 km. We also perform T63L120 and T159L120 to check the T42L60 results. The high resolution results are sufficiently similar to those presented here.

The vertical distribution of the static stability in an initial condition is based on the observations [16]. The lower atmosphere close to the ground is weakly stable. In the cloud layer, there is an almost neutral layer (from 55 to 60 km). At the bottom of the cloud layer it is stable, and static stability has a maximum at around 45 km. Above the cloud layer (above 70 km), it is strongly stratified. It is expected that unstable modes will appear in the cloud layer. In addition, dependence on the static stability is also investigated [12].

The initial condition is an idealized solid body superrotating flow. The flow linearly increases with height from ground to 70 km, which is suggested by the observation [17]. Its maximum is 100 m/s at 70 km at the equator. Above 70 km the velocity is

assumed to be constant. The initial temperature distribution is in balance with the zonally symmetric flow, namely, gradient wind balance. Meridional temperature gradient from equator to pole is about 5 K on a sigma surface at the top of cloud layer. Initiated from this initial condition, the model is integrated for 5 Earth years.

3.3 Results

In the control run in which the solar heating is excluded for simplicity, the superrotation decreases a little in the cloud layer (50 - 70 km) due to unstable modes of growing vortices. Figure 4 shows the horizontal cross sections of snapshots of vorticity disturbances, zonal mean horizontal flow, and zonal mean temperature at 54 km. Clearly, a vortical structure of wavenumber 5 and 6 grows at the middle latitudes. They have significant amplitude later. These growing vortices decrease superrotating flow where they evolve. After they grow to significant amplitude, their horizontal structures change.

Figure 5 shows longitude-height cross sections of meridional flow (a), temperature deviation (b), and vertical flow (c) at 45°N where unstable modes grow at the initial stage of 30 days. The phases of these disturbances are tilted from down-east to up-west. In addition, they are out of phase. That is, while cold air flows downward and southward, warm air flows upward and northward. This is a typical structure of baroclinic instability.

These structures of unstable modes are almost consistent with those reported in the previous linear stability analysis. Since stable layer exists below the cloud layer and density in the lower layer is large, unstable mode does not extend to the lower layer. Next we investigate momentum and heat transport by growing vortices. It is found that zonal flow is accelerated by unstable modes using available potential energy in the initial stage of baroclinic instability. Thus, momentum flux converges to the position where the baroclinic modes develop, and heat flux is negative in the northern hemisphere, that is, heat is transported from equator to pole. In order to examine how baroclinic instability depends on static stability, several vertical distributions of static stability are used. With static stability slightly larger than that assumed in the control run, baroclinic instability does not take place. However, with static stability smaller than that assumed in the control run in the bottom of the cloud layer, baroclinic modes develop and contribute to transport of angular momentum from middle latitudes to equator around 70 km. This momentum transport accelerates the superrotation in the equatorial region.

We also perform simulations with two patterns of solar heating. The zonal mean zonal flows at 1440 days for the runs with the zonally averaged solar heating (a) and with the solar heating with diurnal variation (b) are shown in Fig. 6. There are mid-latitude jets at about 80 km due to meridional circulation

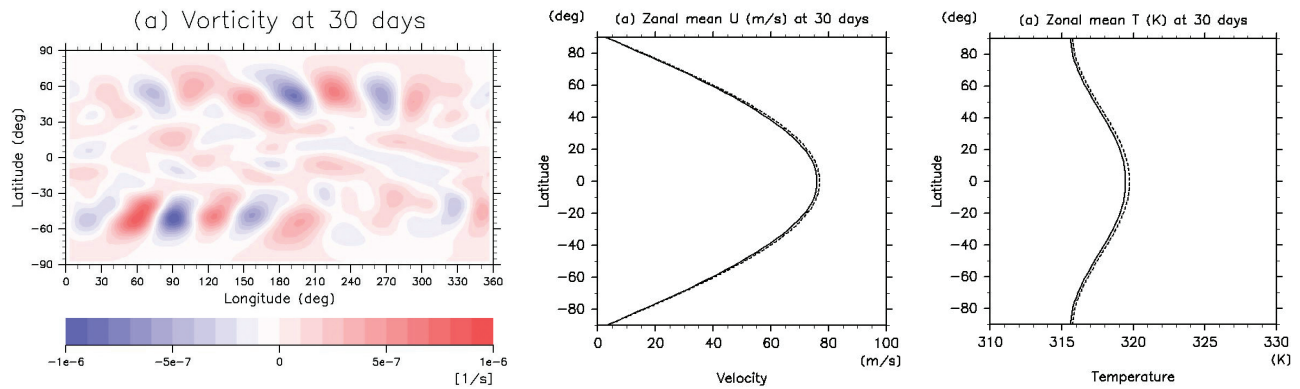


Fig. 4 Snapshots of horizontal cross section of vorticity disturbance (left), latitudinal profiles of zonal mean zonal flow (center) and zonal mean temperature (right) at 54 km at 30 days.

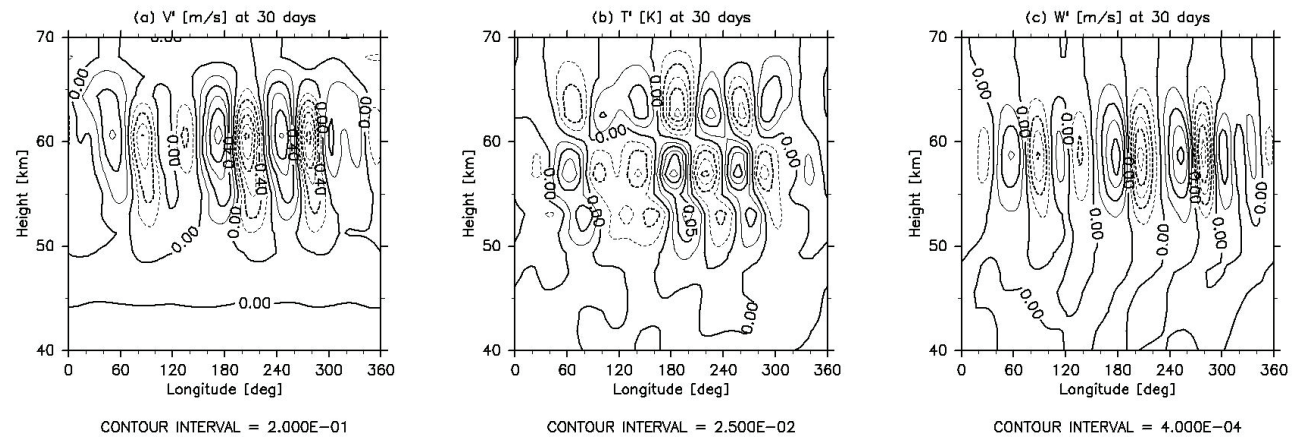


Fig. 5 Longitude-height cross sections at 45°N of meridional flow disturbance (a), temperature disturbance (b), and vertical flow at 300 days.

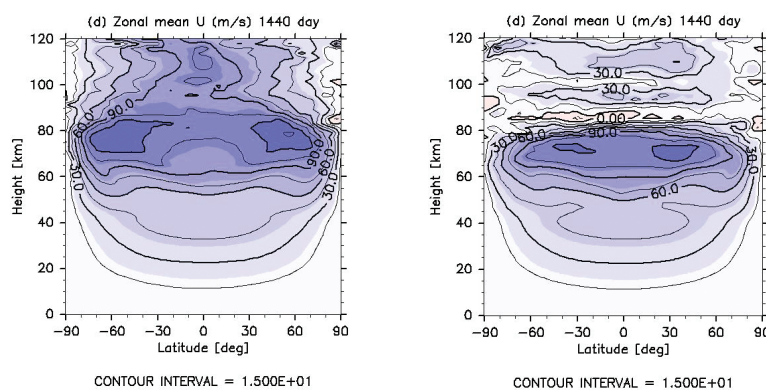


Fig. 6 Latitude-height cross sections of zonal-mean zonal flow for the cases of zonal-mean solar heating (a) and solar heating with diurnal variation (b) at 1440 days.

driven by the zonal-mean solar heating. In contrast, for the run with the diurnal variation the mid-latitude jets are not so clear. Velocity of the zonal-mean zonal flow is almost constant from the equator to the mid-latitudes at about 70 km. Faster superrotation (120 m/s) is generated in this region, while strong deceleration of zonal-mean zonal flow above 80 km is observed, which may be due to thermal tides generated by solar heating, as pointed by the previous study [18]. Further analysis is needed to explain why the superrotation is accelerated.

So far, there are no observations of baroclinic instability on Venus, though they are considered to be important [19]. The present study suggests the baroclinic modes could exist in the Venus cloud layer. It is also expected that the baroclinic modes have a significant impact on the general circulation on Venus through momentum and heat transportation. It is important to take the realistic static stability into account to investigate dynamics at the cloud levels. It is also worthwhile to compare the results with observations brought by Venus Express. Interesting phenomena, such as polar vortices, have been reported in recent years.

Finally, we carried on only short term integrations initiated from superrotating flow in this study. For future work, we plan to perform long time numerical simulations with several experimental configurations. As is frequently discussed on Gierasch mechanism, several unstable modes are candidates to transport momentum from pole to equator [20]. Long time numerical simulations initiated from superrotation would be one of the promising ways to investigate statistical roles of disturbances, including baroclinic modes, on the superrotation. Further study with high resolution simulations and a realistic radiative transfer process may reveal the generation and maintenance mechanism of the Venus atmospheric superrotation.

References

- [1] Ohfuchi, W., H. Nakamura, M. K. Yoshioka, T. Enomoto, K. Takaya, X. Peng, S. Yamane, T. Nishimura, Y. Kurihara, and K. Ninomiya, “10-km Mesh Meso-scale Resolving Simulations of the Global Atmosphere on the Earth Simulator - Preliminary Outcomes of AFES (AGCM for the Earth Simulator)” -, *Journal of the Earth Simulator*, 1, 8, 2004.
- [2] Wilson, R. J. and K. Hamilton, “Comprehensive Model Simulation of Thermal Tides in the Martian Atmosphere”, *J. Atmos. Sci.*, 53, 1290-1326, 1996.
- [3] Takahashi, Y. O., H. Fujiwara, H. Fukunishi, M. Odaka, Y.-Y. Hayashi, and S. Watanabe, “Topographically induced north-south asymmetry of the meridional circulation in the Martian atmosphere”, *J. Geophys. Res.*, 108, 5018, doi:10.1029/2001JE001638, 2003.
- [4] Takahashi, Y. O., H. Fujiwara, and H. Fukunishi, “Vertical and latitudinal structure of the migrating diurnal tide in the Martian atmosphere: Numerical investigations”, *J. Geophys. Res.*, 111, E01003, doi:10.1029/2005JE002543, 2006.
- [5] Newman, C. E., S. R. Lewis, and P. L. Read, “Modeling the Martian dust cycle 1. Representation of dust transport processes”, *J. Geophys. Res.*, 107, 5123, doi:10.1029/2002JE001910, 2002.
- [6] Yamamoto, M. and M. Takahashi, “The fully developed superrotation simulated by a general circulation model of a Venus-like atmosphere”, *J. Atmos. Sci.*, 60, 561-574, 2003.
- [7] Young, R. E., H. Houbel, and L. Pfister, “Baroclinic instability in the Venus atmosphere”, *J. Atmos. Sci.*, 41, 2310-2333, 1984.
- [8] Takagi, M. and Y. Matsuda, “A study on the stability of a baroclinic flow in cyclostrophic balance on the sphere”, *Geophysical Research letters*, 33, L14807, doi:10.1029/2006GL026200, 2006.
- [9] Gierasch, P. J., “Meridional circulation and maintenance of the Venus atmospheric rotation”, *J. Atmos. Sci.*, 32, 1038-1044, 1975.
- [10] Sugimoto, N., M. Takagi, Y. Matsuda, Y. O. Takahashi, M. Ishiwatari, and Y.-Y. Hayashi, “Numerical modeling for Venus atmosphere based on AFES (Atmospheric GCM For the Earth Simulator)”, *System Simulation and Scientific Computing, Communications in Computer and*

- Information Science (CCIS), Springer-Verlag, pp. 70-78, 2012.
- [11] Sugimoto, N., M. Takagi, Y. Matsuda, Y. O. Takahashi, M. Ishiwatari, and Y.-Y. Hayashi, "Baroclinic modes in the atmosphere on Venus simulated by AFES", *Theoretical and Applied Mechanics Japan*, Vol.61, pp. 11-21, 2013.
- [12] Sugimoto, N., M. Takagi, and Y. Matsuda, "Baroclinic instability in the Venus atmosphere simulated by GCM", *J. Geophys. Res.*, submitted. (2013JE004418)
- [13] Sugimoto, N., M. Takagi, Y. Matsuda, Y. O. Takahashi, M. Ishiwatari, and Y.-Y. Hayashi, "Toward high resolution simulation for the atmosphere on Venus by AFES (Atmospheric GCM For the Earth Simulator)", *Proceedings of International Conference on Simulation Technology*, Paper ID: 73 (8 pages), 2012.
- [14] Crisp, D., "Radiative forcing of the Venus mesosphere: I. solar fluxes and heating rates", *Icarus*, 67, 484-514, 1986.
- [15] Tomasko, M. G., L. R. Dose, P. H. Smith, and Odell, A.P., "Measurements of the flux of sunlight in the atmosphere of Venus", *J. Geophys. Res.*, Vol. 85, 8167-8186, 1980.
- [16] Gierasch P. J., R. M. Goody, R. E. Young, D. Crisp, C. Edwards, R. Kahn, D. Rider, A. del Genio, R. Greeley, A. Hou, C. B. Leovy, D. McCleese and M. Newman, "The General Circulation of the Venus Atmosphere: an Assessment", In *Venus II: Geology, Geophysics, Atmosphere, and Solar Wind Environment*. University of Arizona Press, p.459, 1997.
- [17] Shubert, G., "General circulation and dynamical state of Venus atmosphere, In "Venus" (A83-37401 17-91) edited by D. Hilten, University of Arizona Press: Tucson, 681-765, 1983.
- [18] Takagi, M. and Y. Matsuda, "Effects of thermal tides on the Venus atmospheric superrotation", *J. Geophys. Res.*, 11, D09112, doi:10.1029/2006JD007901, 2007.
- [19] Allison, M., A. Del Genio, and W. Zhou, "Zero potential vorticity envelopes for the zonal-mean velocity of the Venus/Titan atmosphere", *J. Atmos. Sci.*, 51, 694-702, 1994.
- [20] Iga, S. and Y. Matsuda, "Shear instability in a shallow water model with implications for the Venus atmosphere", *J. Atmos. Sci.*, 62, 2514-2527, 2005.

AFES を用いた地球型惑星の大気大循環シミュレーション

プロジェクト責任者

林 祥介 神戸大学 大学院理学研究科

著者

林 祥介^{*1}, 高橋 芳幸^{*1}, 杉本 憲彦^{*2}, 高木 征弘^{*3}, 石渡 正樹^{*4}, 小高 正嗣^{*4},
竹広 真一^{*5}, 中島 健介^{*6}, はしもとじょーじ^{*7}, 松田 佳久^{*8}

*1 神戸大学 大学院理学研究科

*2 慶應義塾大学 自然科学研究教育センター

*3 東京大学 大学院理学系研究科

*4 北海道大学 大学院理学研究院

*5 京都大学 数理解析研究所

*6 九州大学 大学院理学研究院

*7 岡山大学 大学院自然科学研究科

*8 東京学芸大学 教育学部

大気大循環モデル AFES (AGCM (Atmospheric General Circulation Model) for the Earth Simulator) に基づく GCM を用いて、火星大気の高解像度大気大循環シミュレーションを実施した。加えて、これまでに開発してきた高精度の金星大気放射モデルを用いた高解像度シミュレーションの準備として、簡単な物理過程を用いた中解像度での大気大循環シミュレーションを実施した。我々の研究の目的は、地球型惑星大気における中小規模擾乱の力学的特徴と、その大気大循環への影響を調べることである。火星大気シミュレーションは、非常に高い解像度で実施した。高解像度モデル (T319L96) と中解像度モデル (T79L96) を用いた長期間シミュレーションの結果、両者は擾乱の表現に差がありながらも、ダスト巻き上げの起こる緯度と季節が定性的に同様であった。しかし、予想されるように、ダスト巻き上げ領域は高解像度モデルの方が広い。このことは、小規模擾乱が大気中のダスト量の決定において重要な役割を果たすことを示唆している。また、金星大気シミュレーションに関しては、現実的な太陽加熱の基でスーパーローテーションが長時間維持された。また、安定度の小さい雲領域では、傾圧不安定が発達した。これら傾圧不安定の初期の構造は線形安定性解析で示されたものと同様であるが、その時間発展では水平構造の変化も見られた。これら傾圧不安定による運動量と熱の南北輸送についても調べた。本研究の結果は、(1) 静的安定度の鉛直分布が傾圧不安定の発生に不可欠であること、(2) 金星大気中で、これまでの研究では再現されていない傾圧不安定が起こりうること、(3) 傾圧不安定が金星大気大循環において重要な役割の一つを果たす可能性があること、を示唆している。

キーワード: 惑星大気, スーパーローテーション, ダストストーム, 地球, 火星, 金星